Environ. Sci. Technol. **2000**, *34,* 192−198

Surfactant-Enhanced Partitioning of Nickel and Vanadyl Deoxophylloerythroetioporphyrins from Crude Oil into Water and Their Analysis Using Surface-Enhanced Resonance Raman Spectroscopy

RICARDO CANTÚ,[†,‡] JOSEPH R. STENCEL,[§] ROMAN S. CZERNUSZEWICZ,[*,†] PETER R. JAFFÉ,[§] AND TIMOTHY D. LASH[||]

Department of Chemistry, University of Houston, Houston, Texas 77204, Department of Civil Engineering and Operations Research Environmental Engineering and Water Resources Group, Princeton University, Princeton, New Jersey 08544, and Department of Chemistry, Illinois State University, Normal, Illinois 61790

The authors have addressed the identification of molecular fossils of deoxophylloerythroetioporphyrin (DPEP) complexes of vanadium (V) and nickel (Ni) and its partitioning from crude oil into the environment. The analyses described here involve water/surfactant solutions that were in contact with the Boscan crude oil for 1 month. Both VO(DPEP) and Ni(DPEP) are identified using resonance Raman (RR) and surface-enhanced resonance Raman (SERR) spectroscopies. Synthetic metalloporphyrins (petroporphyrins) are employed as standards for fingerprinting the naturally occurring crude oil pigments. Supplementary analyses of the Boscan crude oil (source) using inductively coupled plasma (ICP) and ultraviolet−visible (UV−Vis) spectroscopies along with ionic monitoring of the water samples using UV−Vis, ICP, and ion chromatography (IC) were used to assist in establishing their relative abundance and multiple speciation porphyrin forms in the aqueous environment. Results showed that partitioning of V and Ni from the oil phase to the aqueous phase is extremely low and that most of the V and Ni in the aqueous phase is not in ionic form. Although direct partitioning of these metals into the water phase from the oil phase is low, surfactants increase this partitioning of the metalloporphyrin chelates into the water. The results of this study have shown that contamination of drinking water by metals released from crude oils through partitioning is small, and the metals in the aqueous phase are primarily in a complexed form, which further reduces toxicity concerns. Under certain circumstances, it is likely that humic substances, like surfactants, may enhance the partitioning of these complexed metals.

Introduction

The spilling of large quantities of crude oil to the environment, either intentionally (e.g., Kuwait spills of 1990) (*1*) or unintentionally [e.g., pipeline breaks in Bemidji, MN (*2*), or the Valdez oil tanker accident, etc.), has the potential to impact surface water and groundwater supplies with toxic levels of metals. Speight (*3*) gives a range of concentrations of trace metals found in crude oil. Nickel and vanadium are the most abundant of these trace metals. The concern for vanadium and nickel has been from the standpoint of "poisoning" zeolite-containing cracking catalyst (*4*) but never from an environmental perspective. In recent years, several authors (*5, 6*) have shown that the ratio of vanadium to nickel can be utilized as a biomarker with environmental measurement potential. Very little study has been given to the potential leaching of these metals from the oil phase to the environment or if it may create toxic levels in groundwater. Our present research indicates that while the partitioning may be expected to be very small, it is indeed taking place and may be of concern for larger spills of specific types of crude oil or for chronic spills around some types of facilities. In addition, low-level detection methods, i.e., parts per trillion (ppt), have only been element specific and not species specific. Our research has focused on detection methods that can be utilized to address the main questions of trace metal concern for large oil spills, i.e., potential contamination of the environment and identification of the species. These detection methods can also be applied to incidents concerning other hazardous materials where transition metals may be involved.

Metalloporphyrins are fairly ubiquitous in nature, particularly iron porphyrins (hemes), which are the prosthetic groups for the cytochromes, hemoglobin, etc., and magnesium dihydroporphyrins or chlorophylls (*7*). Nickel(II) and oxo-vanadium(IV) complexes of deoxophylloerythroetioporphyrin (DPEP) (Figure 1) dominate petroleum, oil shales, and maturing sedimentary bitumen (*8*−*10*). The concentrations of both vanadium and nickel have been shown to vary for different type of oils and related marine depositional environments (*11*). In general, it is believed that only 10% of the total metal in a crude oil is accommodated as porphyrin complexes (*12*), although there is a report that indicates that over 40% of the vanadium and nickel are present as metal porphyrin complexes in Boscan crude oil (*13*). The remaining portion is expected to be in the form of oxides such as NiO, VO, and ash (*8*). Nickel porphyrins are commonly more abundant than vanadium in light crude oils, and the reverse is generally the case for heavy crude oils (*8*).

What is not clear is whether water as a polar solvent has the ability to partition appreciable amounts of these trace metals from the oil, whether aging of the crude has an effect, or whether the species liberated will affect the transport properties of the metals through porous media.

Vanadium does not have a mean contamination limit (MCL) in accordance with either the U.S. Environmental Protection Agency (U.S. EPA) safe drinking water regulations or the World Health Organization (WHO) standards. Vanadium is, however, on the the U.S. EPA regulatory list for consideration. The MCL of 100 ppb for nickel was remanded by the U.S. EPA in 1995. At present, there is no indication that it will come back onto the regulatory docket soon. In

* Corresponding author phone: (713)743-3235; fax: (713)743-2709; e-mail: Roman@uh.edu.

[†] University of Houston.

[‡] Present address: Microbiological and Chemical Exposure Assessment Research Division, National Exposure Research Laboratory, U.S. Environmental Protection Agency, Cincinnati, OH 45268.

[§] Princeton University.

[||] Illinois State University.

10.1021/es990213s CCC: $19.00
Published on Web 11/23/1999

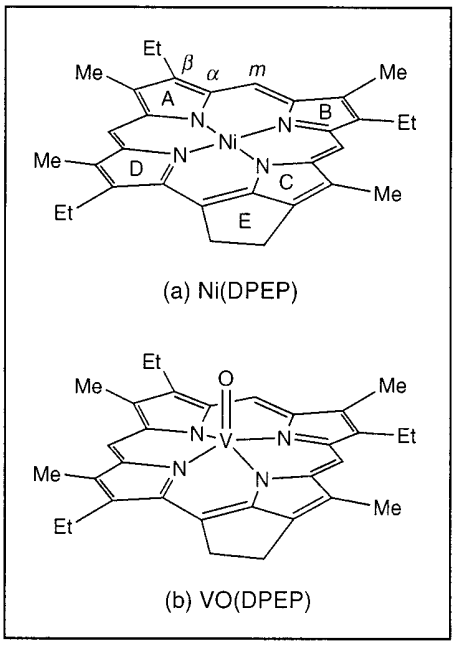

FIGURE 1. Structural diagrams of naturally occurring crude oil (a) nickel and (b) vanadium complexes of deoxophylloerythroetioporphyrin (DPEP).

Kuwait where vanadium and nickel were seen in groundwater, Kuwait researchers have been quite interested in drinking water standards and whether the WHO will set a limit in the future for these two metals (*14*).

The octanol/water partitioning coefficient (K_{ow}) is hard to calculate for porphyrins, even using the simple fractionation method discussed by Lyman et al. (*15*) or methods discussed by Reinhard and Drefahl (*16*). An indirect determination, based on the enhancement partitioning in the presence of a surfactant solution, is discussed below. Our research has shown that surfactants, by increasing the solubility of the metal porphyrins in water, do provide an enhanced partitioning mechanism for the metal porphyrins. This implies a potential problem in the environment and also may affect thinking on surfactant cleanup scenarios.

Resonance Raman (RR) spectroscopy has been advantageous in elucidating the structure of geological porphyrins (*17*−*21*). When coupled with the surface-enhanced Raman (SER) effect (*22*), this structural tool has become sufficiently sensitive for the study of transformation products in sedimentary organic matter (*23*). Besides an increased sensitivity, the SER effect efficiently quenches fluorescence, which is frequently a major obstacle in monitoring the analyte of interest in the RR experiments. As a result, the surface-enhanced resonance Raman (SERR) scattering can be used for tracking these molecular fossils in water samples at the ppb level (*23*).

Our study consists of four parts: first, the metal content and DPEP evidence in the Boscan crude oil is examined using inductively coupled plasma (ICP) and ultraviolet−visible (UV−Vis) spectroscopies. Second, water/surfactant samples are analyzed using UV−Vis, ICP, and ion chromatography (IC) methods. Third, RR and SERR scattering techniques are used in an effort to monitor mixtures of nickel and vanadyl cycloalkanoporphyrins (CAPs) using the porphyrin (Soret band) resonant excitation wavelength at 413.1 nm. Finally, off-resonance excitation at 457.9 nm extends and validates the structural fingerprinting of these molecular fossils. The results fingerprint both Ni(DPEP) and VO(DPEP), establish their relative abundance, and detect their multiple speciated forms in the aqueous environment.

Experimental Section

Materials. Boscan crude oil with a nickel content of 95 ppm and vanadium content of 1023 ppm was obtained (Petroleos de Venezuela and the Savannah, GA, CITGO refinery) and metal content verified by an ICP procedure (Huffman Laboratories, Inc., Golden, CO). Extraction of Boscan crude DPEP fractions was carried out as described in the Supporting Information (see paragraph at end of paper). The syntheses of free-base DPEP are described elsewhere (*24*−*26*). Metal insertion was accomplished by reacting the free-base DPEP with either nickel acetate, $Ni(CH_3COO)_2{\cdot}4H_2O$, or vanadyl sulfate, $VOSO_4{\cdot}3H_2O$, to give the corresponding Ni(DPEP) or VO(DPEP) according to the method of Adler et al. (*27*). A set of aqueous surfactant solutions was prepared ranging from 0 to 160 mg/L of Brij-35 surfactant (polyoxyethylene 23 lauryl ether). Four grams of Boscan crude oil was coated on the inside of a 50-mL glass batch reactor to which 50 mL of the surfactant solution was added. These samples were tumbled for 1 month at a constant temperature of 20 °C. The aqueous phase was removed and analyzed. A sequential run was then performed by replenishing the surfactant solution using the same oil samples from the first run. The sequential run followed the same procedure of being tumbled for 1 month and the aqueous phase removed and analyzed.

Methods. A Dionex DX-500 ion chromatography (IC) unit was used for quantifying the ionic fraction of metals (*28*, *29*) partitioned to the water from the Boscan crude oil (*30*). The absorption spectra of the water samples and synthetic petroporphyrins were obtained with a 1-cm quartz cell using a Varian Cary 50 UV−Vis spectrophotometer. Raman excitation was provided by a Coherent K-2 Kr^+ (413.1 nm) or a Coherent 90−6 Ar^+ (457.9 nm) ion laser. The synthetic metalloporphyrins for RR measurements were dissolved in spectroscopic grade dichloromethane. A procedure developed by Schneider et al. (*31*) was used to prepare the silver hydrosols for SERR measurements. Both RR (synthetic DPEPs) and SERR (water samples) spectra were obtained from spinning the samples in NMR tubes positioned in 135° backscattering geometry. The scattered photons were collected and analyzed by a SPEX 1403 double monochromator coupled to a Hamamatsu 928 photomultiplier detector (*32*). A more detailed description of the experimental methods is given in the Supporting Information.

Results

Metal Content and DPEP Evidence in the Boscan Crude Oil. The ICP analysis of the Boscan crude reveal 1023 ppm of vanadium and 95 ppm of nickel. This crude oil is evidently rich in vanadium porphyrins as shown in Figure 2a. All of the chromatographic bands eluted (see Supporting Information) were consistent with this spectrum. The bands at 410.5, 533.6, and 574.3 nm (Table 1) correspond notably well to three classical metalloporphyrin absorptions (*33*): a very strong band (Soret) near 400 nm and two weaker *Q* bands in the range of 500−600 nm. This is confirmed as we compare the crude oil absorptions to the synthetic VO(DPEP) in Figure 2b. Vanadium porphyrins occur in the form of vanadyl (VO^{2+}) porphyrins (*9*) and will be referred to as vanadium throughout this work to encompass both ionic and molecular studies. In Ni(DPEP), the porphyrin absorptions blue-shift to 393.6, 513.7, and 552.7 nm (Table 1). These shifts, which are expected with increased planarity of the porphyrin macrocycle (*34*, *35*), were not readily observed in any of the isolated crude oil bands (Figure 2a). This behavior supports qualitatively the ICP data, which indicated more abundant vanadium than nickel from the Boscan source.

UV−Vis, ICP, and Ionic Monitoring of the Water Samples. A water/surfactant solution was in contact with

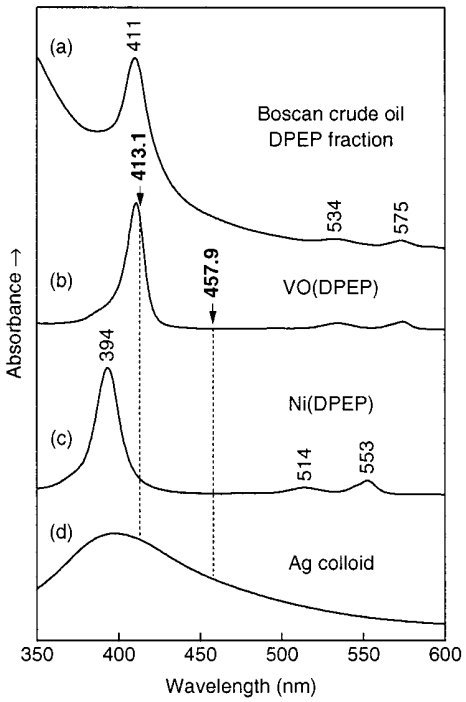

FIGURE 2. UV−Vis absorption spectra of (a) Boscan crude oil extract and (b, c) indicated petroporphyrin standards in dichloromethane and (d) a silver hydrosol used in SERR analyses of water samples. Laser excitation lines (413.1 and 457.9 nm) are indicated.

TABLE 1. UV−Vis Absorption Maxima (nm) and Molar Absorptivities (cm^{-1} M^{-1}) for DPEP Petroporphyrins[a]

	Ni(DPEP)		VO(DPEP)	
band	λ_{max}	ϵ_{max}	λ_{max}	ϵ_{max}
Soret	393.6	1.45×10^5	410.5	1.28×10^5
Q_1	513.7	8.40×10^3	533.6	7.06×10^3
Q_0	552.7	1.66×10^4	574.5	8.72×10^3

[a] All data are from UV−Vis spectra of dichloromethane solutions. The ϵ_{max} values were obtained from the slopes of the plots of absorbance versus petroporphyrin concentration (not shown). Stock solutions of 0.76 mM Ni(DPEP) and 0.61 mM Ni(DPEP) were used. Five solutions with petroporphyrin concentration range of 1−16 μM were prepared by dilution of stock solutions, which gave absorbances in the range of 0.5−2.5.

the Boscan source for 1 month (see Experimental Section). UV−Vis spectra of the water samples did not give any spectral features of either ionic or molecular species apparently because the concentrations of the metal ions partitioned into the water were very low. The analysis of these water samples via ICP indicated an enhancement by the surfactant of the partitioning of vanadium between the oil and water phase as shown in Figure 3. Assuming that the enhancement of the partitioning and/or solubilization of a hydrophobic organic by a given surfactant is proportional to the organic compound's K_{ow}, we can compare the results shown in Figure 3 to the enhanced solubilization of phenanthrene by the same surfactant as shown by Guha and Jaffé (*36*), to estimate a value of K_{ow} for the complexed vanadium. This procedure considers the following calculations:

$$C_{mic} = S_{mic} k_{mic} C$$

$$S_{mic} = S - \text{cmc for } S > \text{cmc}$$

$$S_{mic} = 0 \text{ for } S > \text{cmc}$$

where C_{mic} is the vanadium partitioned into micelles (ppb),

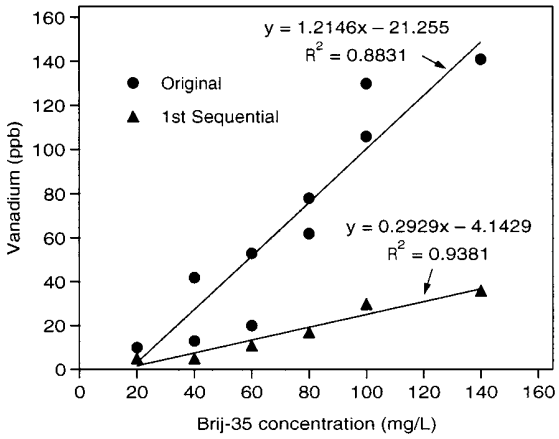

FIGURE 3. Vanadium partitioning between Boscan crude oil and water of various Brij-35 surfactant concentrations.

C is the vanadium truly dissolved in the water (ppb), S is the total surfactant concentration (mg/L), S_{mic} is the surfactant concentration in micelle form (mg/L), cmc is the critical micelle concentration (mg/L), and k_{mic} is the partition coefficient of vanadium between the micellar and aqueous phases (L/mg). Then, for our vanadium analysis:

$$k_{mic} = \frac{C_{mic}}{S_{mic} C} = 0.15 \text{ L/mg}$$

For phenanthrene (C_6H_{10}), the log (K_{ow}) = 4.46 and k_{mic} = 0.0144 L/mg (*36*). Using a ratio of

$$\frac{k_{mic(phen)}}{K_{ow(phen)}} = \frac{k_{mic(porph)}}{K_{ow(porph)}}$$

then

$$K_{ow(porph)} = \frac{k_{mic(porph)} K_{ow(phen)}}{k_{mic(phen)}} = \frac{0.15 \times 10^{4.46}}{0.0144} = 10^{5.47}$$

or log (K_{ow}) = 5.47 for the VO(DPEP), if we assume essentially all of the vanadium is as VO(DPEP). This method appears to be a reasonable calculation based on the work of Guha and Jaffé (*37*) when micellar partition coefficients of naphthalene, phenanthrene, and pyrene are compared to K_{ow}. The water samples at 80 mg/L of Brij-35 gave 78 and 17 ppb of vanadium, respectively, for the original and sequential runs (ICP analysis). Since the content of nickel is an order of magnitude smaller than vanadium in the Boscan crude oil, a value of less than 10 ppb would be expected for the nickel in the water phase.

The IC analysis indicated ionic nickel partitioning into the water matrix from the crude oil at approximately 1−1.5 ppb while vanadium in the ionic form was undetectable, indicating a value of less than 0.5 ppb. A burning technique (900 °C) also provided some evidence of vanadium partitioning in a potential porphyrin phase (*30*), but this has given too much variability to be a reliable technique. The negligible ionic detection of both metal ions led us to assume that these were in a complexed form, possibly with porphyrins.

VO(DPEP) Raman Marker Bands in the Water/Surfactant Samples. Figure 4 shows the Soret excitation (413.1 nm) SERR spectra of the two Boscan water samples having different contents of vanadium and nickel: 78 ppb V, <10 ppb Ni (trace 4d); 17 ppb V, <2 ppb Ni (trace 4e). The CH_2Cl_2 solution RR spectra of pure VO(DPEP) (trace 4a) and Ni(DPEP) (trace 4b) as well as their mixture with a concentration ratio $R_{Ni/VO}$ = [Ni(DPEP)]/[VO(DPEP)] = 1.25 (trace 4c) are also included

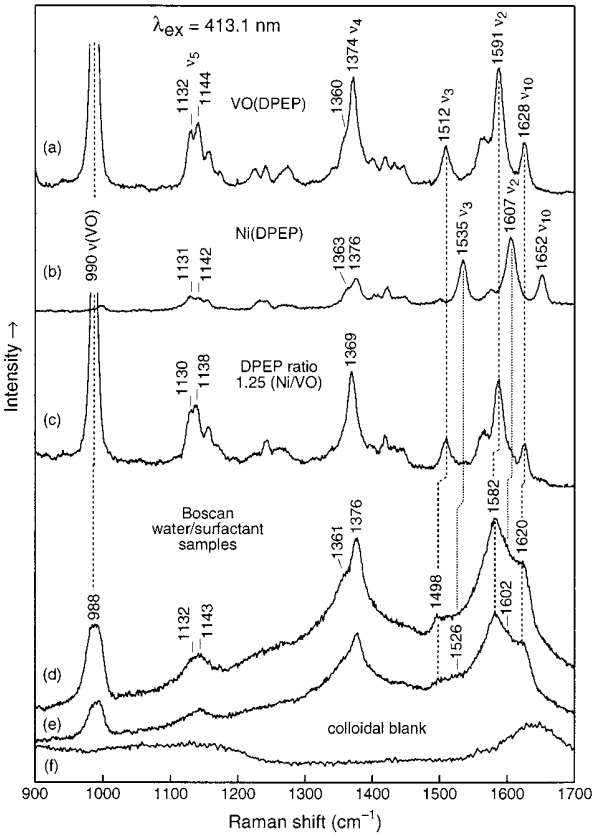

FIGURE 4. 900−1700 cm^{-1} SERR spectra of two Boscan water/surfactant samples: (d) original, 78 ppb vanadium, <10 ppb nickel; (e) sequential run, 17 ppb vanadium, <2 ppb nickel. Both spectra taken from silver hydrosols (f) with Soret band excitation (413.1 nm). The corresponding RR spectra from CH_2Cl_2 solutions of pure VO(DPEP) (a) and Ni(DPEP) (b) and their mixture of $R_{Ni/VO} = 1.25$ (c) are shown. The DPEP Raman marker bands are correlated by dashed (vanadium) and dotted (nickel) lines.

for fingerprinting purposes of the possible porphyrins partitioned into the water. The observed Raman marker bands ν_2, ν_3, ν_4, ν_5, and ν_{10} of Ni(DPEP) and VO(DPEP) are listed in Table 2. These bands arise from the in-plane porphyrin skeletal vibrations (*20, 21*), their distinctive spectral positions allowing for easy differentiation between the two metals (*17*). Another unique feature in the Soret excitation RR and SERR spectra is the oxo-vanadium stretching, ν(VO), near 990 cm^{-1} that is characteristic of vanadyl porphyrins in the 950−1050 cm^{-1} region (*17, 38*).

The RR spectrum with $R_{Ni/VO} = 1.25$ (Figure 4c) appears to fit surprisingly well the enhancement pattern seen in 413.1 nm excited SERR spectra of the water samples analyzed (traces 4d and e). Clearly, the vanadyl porphyrin vibrations are the major contributors to these spectra. Figure S.1, found in the Supporting Information, shows that even when the $R_{Ni/VO} = 6.23$, the ν_2 vibration of VO(DPEP) remains relatively more strongly enhanced than its Ni(DPEP) correspondent. In general, this dominance of vanadyl porphyrin bands under 413.1 nm excitation is explained on the basis of its proximity (*32*) to the porphyrin Soret absorption band. The Soret transition of VO(DPEP) at 410.5 nm is only 2.6 nm distant to the 413.1 nm laser wavelength, but that of Ni(DPEP) at 393.6 nm is farther away with a 19.5 nm separation (Figure 2). At this point, it was not clear why these petroporphyrins seem to be present in an almost 1:1 ratio since the preliminary ICP analysis indicated 78 ppb of vanadium and less than 10 ppb of nickel. This situation suggests that 10 ppb or less of vanadium was detected in the SERR spectra while the remaining vanadium was not. The synthetic VO(DPEP) Raman marker bands at 1628 (ν_{10}), 1591 (ν_2), and 1512 cm^{-1} (ν_3) correspond well to those at 1620 (ν_{10}), 1582 (ν_2), and 1498 cm^{-1} (ν_3) of the water samples. This information is summarized in Table 2. The $R_{Ni/VO} = 1.25$ is assumed after noticing the ν_2 and ν_3 markers at 1607 and 1535 cm^{-1} (Figure 4c), which belong to Ni(DPEP) (trace 4b). Their correspondents are observed as weak shoulders near 1602 and 1526 cm^{-1} in the water samples (traces 4d and e).

TABLE 2. Raman Marker Bands (cm^{-1}) for DPEP Detection of Nickel and Vanadyl Complexes in Crude Oils and Water Samples

		Ni(DPEP)			VO(DPEP)		
marker	description[a]	synthetic[b]	water[c]	Δ[d]	synthetic[b]	water[c]	Δ[d]
ν_{10}	$\nu(C_\alpha C_m)_{asym}$	1652	1642	−10	1628	1620	−8
ν_2	$\nu(C_\beta C_\beta)$	1607	1602	−5	1591	1582	−9
ν_3	$\nu(C_\alpha C_m)_{sym}$	1535	1526	−9	1512	1498	−14
ν_4	ν(Pyr half-ring)	1376	1376	0	1374	1376	+2
ν_5	$\nu(C_\beta C_1)$	1142			1144	1143	−1
		1131			1132	1132	0
ν(VO)	vanadyl stretch				990	988	−2
						977[e]	−13

[a] See refs *48* and *49* for mode descriptions. Porphyrin carbon labels α, *m*, and β are given in Figure 1. [b] RR frequencies of petroporphyrin standards in dichloromethane. [c] SERR bands for petroporphyrins in the original water/surfactant colloidal sample (78 ppb V, <10 pbb Ni). [d] Observed Raman shifts include solvent, colloidal, and surfactant interactions. [e] This value corresponds to 5-coordinate hydrogen-bonded oxo-vanadium vibration observed in 1-year-old water/surfactant samples (spectra not shown).

Careful examination of the ν_4 marker band near 1375 cm^{-1} (Figure 4) becomes important in distinguishing the DPEP structural type from etioporphyrins (Etios), the other most abundant petroporphyrin type (*39*). This class of petroporphyrins lacks the exocyclic ring E at the porphyrin periphery. This ν_4 vibration has been shown to be very strong and dominating in etioporphyrin RR spectra with Soret resonant excitation and occur at 1380 and 1377 cm^{-1} for geological Ni(Etio-III) and VO(Etio-III), respectively (*17*). In contrast, the DPEP type petroporphyrins show a less enhanced ν_4 vibration next to a porphyrin alkyl band (*21*). VO(DPEP) shows the ν_4 peak at 1374 cm^{-1} with a moderate shoulder at 1360 cm^{-1} (trace 4a), while Ni(DPEP) exhibits these bands at 1376 and 1363 cm^{-1}, respectively (trace 4b). In the DPEP mixture, the ν_4 band collapses into a poorly resolved singlet centered at ~1369 cm^{-1}. The water samples (traces 4d and 4e) display this spectral feature at 1376 cm^{-1} with a clearly visible shoulder at 1361 cm^{-1}, further suggesting that the metals are complexed to DPEP.

Attention to the intensities of the ν_5 bands at 1132 and 1144 cm^{-1} in VO(DPEP) (Figure 4a) gives supplementary evidence to the detection of vanadyl porphyrin. The 1144 cm^{-1} peak is more intense in this pair. In contrast, the relative intensities of the ν_5 bands at 1131 and 1142 cm^{-1} are reversed in Ni(DPEP), with an overall marked loss of enhancement in this region (trace 4b). Consequently, the DPEP mixture (trace 4c) yields a pair of ν_5 bands that is very similar to VO(DPEP). In SERR spectra of the water samples (traces 4d and e), the ν_5 bands appear as a broad feature at ~1143 cm^{-1} and a weaker shoulder at ~1132 cm^{-1}, which further supports vanadyl porphyrin existence in the aqueous samples.

Most conspicuous, however, is a strong appearance of the characteristic vanadyl stretch, ν(VO), at 988 cm^{-1} in SERR spectra upon addition of the water samples to the Ag hydrosols, even though its intensity has markedly diminished relative to the porphyrin skeletal bands (traces 4c and d). SERR scattering is observed whenever a scattering species is located at or in vicinity of the Ag colloid surface (*22*). The Brij-35 surfactant here can act as a molecular spacer between

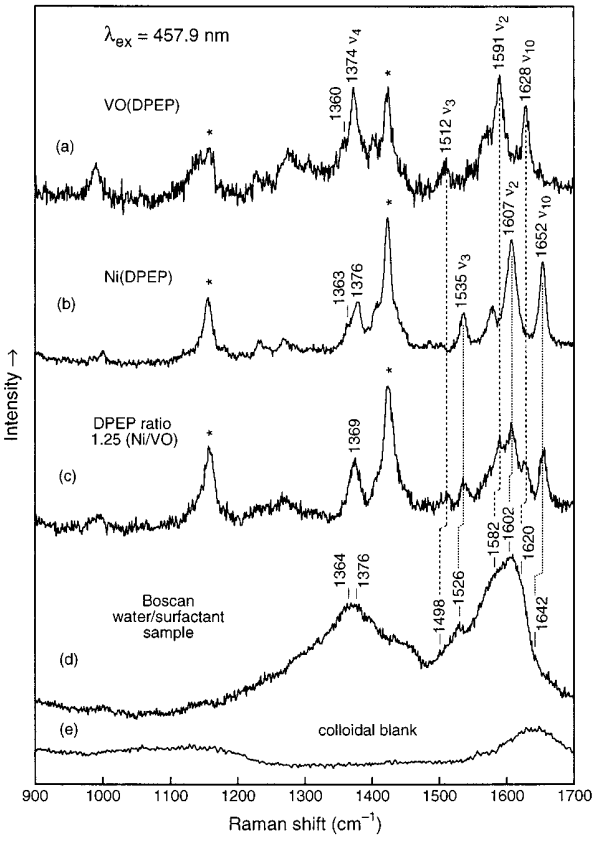

FIGURE 5. Same as Figure 4 but with off-Soret band excitation (457.9 nm) and for the original water (78 ppb vanadium, <10 ppb nickel) sample only. Asterisks indicate CH_2Cl_2 solvent bands.

the silver colloid and the metalloporphyrins (*40, 41*), with its hydrophilic and hydrophobic parts interacting with the colloid surface and the porphyrin macrocycle, respectively. We suggest the metalloporphyrin intercalates to the aliphatic tail of the surfactant ($C_{12}H_{25}$). This intercalation promotes weakening of porphyrin π conjugation, as evident by downshifting of the several Raman marker vibrations (Table 2). Apparently, it also allows a proper orientation of the porphyrin macrocycle with respect to the Ag surface for SERR enhancement of the in-plane skeletal vibrations. In contrast, the oxo-vanadium vibration in the water samples gives a much weaker SERR ν(VO) peak as compared to its RR counterpart of synthetic VO(DPEP) in CH_2Cl_2 for several reasons. Vanadyl porphyrins are expected to be domed (*42*). This oxo-metal vibration is expected to orient out of the plane of the porphyrin structure (which is intercalated to the surfactant). Therefore, the ν(VO) vibration does not receive much benefit from the SERR effect derived from the silver colloid.

Ni(DPEP) Raman Marker Bands in the Water/Surfactant Samples. Because the oxo-vanadium vibration (strongest band in the 413.1 nm spectra) derives its intensity from the porphyrin Soret electronic transition (*38*), it is expected to be considerably reduced in intensity when the porphyrin excitation wavelength is sufficiently distant from the Soret peak maximum. As shown in Figure 5 (trace 5d), the 457.9 nm excitation SERR spectrum taken from the original water sample confirms this expectation. This experimental evidence is consistent with the RR spectra of pure VO(DPEP) and the DPEP mixture = 1.25 (Ni/VO) (traces 5a and c). Note carefully that several other features not readily observed in the 413.1 nm SERR spectra complicate the high-frequency region above 1500 cm^{-1} of the water sample excited at 457.9 nm (trace 5d). Again, changes seen in this region are consistent with the RR spectrum of the $R_{Ni/VO} = 1.25$ mixture (trace 5c). The vanadium Raman marker bands ν_2, ν_3, and ν_{10} are found at ~1498, ~1582, and ~1620 cm^{-1}, respectively. This Raman signature of VO(DPEP) in water was confirmed earlier by the SERR spectra at 413.1 nm excitation (Figure 4). The new additions to the SERR spectrum in Figure 5d are seen at ~1526, ~1602, and ~1642 cm^{-1} (tentative) and can be traced back as the downshifted ν_2, ν_3, and ν_{10} nickel Raman marker bands (Table 2).

At this point, it was not clear why the skeletal modes of Ni(DPEP), most markedly ν_2, were enhanced more than those in VO(DPEP) using the 457.9 nm laser line, as this excitation wavelength is farther (~64 nm) removed from resonance with the Soret peak maximum for Ni(DPEP) than VO(DPEP) (~47 nm) in Figure 2. Considering these spectral separations, the vanadium porphyrin was predicted to be a dominant contributor to the Raman spectrum excited at 457.9 nm as well. However, one must also consider (*32*) the oscillator strength of the two chromophores in estimating the RR scattered intensity—in general, the higher the oscillator strength of the electronic transition and the closer the laser line to the wavelength of this transition, the more intense the RR scattering (*32*). The molar absorptivity (ϵ) measures this physical property, and we consequently have determined the values of ϵ for Ni(DPEP) and VO(DPEP) absorption bands (ϵ_{max}) as illustrated in Table 1. Indeed, the results show that Ni(DPEP) is a stronger absorber of visible light than VO(DPEP), as evidenced by its Soret band molar absorptivity of 1.45×10^5 M^{-1} cm^{-1} as compared to 1.28×10^5 M^{-1} cm^{-1} for VO(DPEP). Even the two weaker *Q* bands of Ni(DPEP) gave higher ϵ_{max} values as compared to the vanadium complex (Table 1). The 457.9 nm excitation data clearly shows that the ϵ_{max} of the resonant Soret electronic transition becomes an increasingly important factor as the laser excitation wavelength is tuned farther away from the transition wavelength. This conclusion is supported by Figure S.1 found in the Supporting Information; it can be seen there that the 457.9 nm Raman spectra of the CAP mixtures in CH_2Cl_2 exhibit high-frequency marker bands of the stronger chromophore nickel chelate that prevail over those of the vanadium complex for most of the mixtures (traces S.1k–q).

Discussion

Our results show both metalloporphyrin species partition into the water/surfactant phase from the oil phase almost in a 1:1 proportion ($R_{Ni/VO}$ = 1.25) estimated using SERR spectroscopy with 413.1 and 457.9 nm excitation wavelengths. This ratio is not in agreement with the ICP analyses that yielded 78 ppb of vanadium and less than 10 ppb of nickel. This discrepancy most likely arises from two effects: (i) the conformation of the metalloporphyrin macrocycle and (ii) the affinity of the central metal ion, especially VO^{2+}, to ligate exogenous ligands and to form hydrogen bonds. Ni(DPEP) is known to be a more planar porphyrin (*43*) than VO(DPEP) (*42*). Hydrogen bonding is not expected to occur since nickel(II) forms stable four-coordinate complexes (*44*). Thus, the nickel porphyrin structure can intercalate very efficiently to the hydrophobic part of the surfactant which is adsorbed on the Ag colloidal surface. The enhancement inherent from the Ag particles is selectively detected upon the 457.9 nm porphyrin excitation.

In contrast, VO(DPEP) is expected to exhibit a domed conformation as the oxo-vanadium bond is sterically projecting out from the center of the porphyrin ring (*42*). This geometrical assembly promotes intercalation only from the porphyrin structure, which may have opposing forces caused by the central metal ion. Namely, the vanadyl group of VO(DPEP) may undergo additional proximal (i.e., at the vanadium site) and distal (i.e., at the oxo group site) interactions with the surrounding molecules in the water/

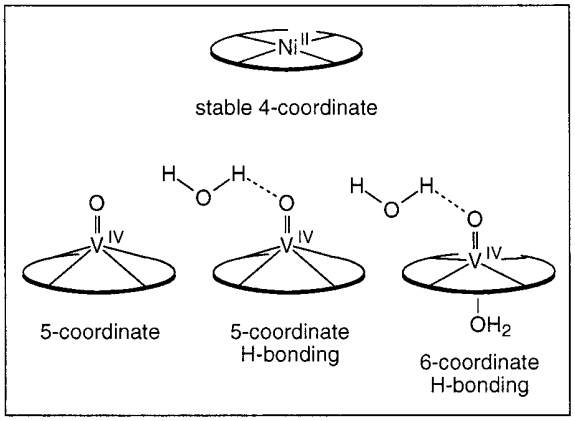

FIGURE 6. Diagramatic representation of various possible Ni(DPEP) and VO(DPEP) species in Boscan water/surfactant samples.

surfactant environment, as illustrated diagrammatically in Figure 6. The ν(VO) stretch at 990 cm^{-1} seen in the CH_2Cl_2 solution RR spectrum of VO(DPEP) is characteristic of five-coordinate species (*17*,*38*). Boscan water/surfactant colloidal samples give this vibration at a similar frequency, 988 cm^{-1}, suggesting that the VO(DPEP) molecules capable of accessing the SERR-active Ag surface are mainly five-coordinated. However, other forms may also be present there as inferred by the broadness and flatness of the 988 cm^{-1} ν(VO) peak and by an additional shoulder that we observed at 977 cm^{-1} in aged water samples (Table 2). This last feature (977 cm^{-1}) corresponds to a hydrogen-bonded five-coordinate vanadyl species (*45*). Therefore, the apparently missing VO(DPEP), indicated by the ICP data, is expected to form six-coordinate species in the bulk of the aqueous solution. Surfactant and water molecules can compete for the oxo-vanadium porphyrin through (i) aliphatic affinity to the porphyrin structure and (ii) hydrogen bonding to the oxo group and axial ligation to the vanadium. This second competing factor may prevent a significant amount of VO(DPEP) from intercalating efficiently to the colloidal/surfactant particle that is used as a detection platform for SERR scattering. Control SERR experiments involving, for example, water-soluble vanadyl porphyrins such as VO(PPIX) (PPIX = protoporphyrin IX) should prove useful in supporting this suggestion and may provide data regarding the degree of VO(DPEP) speciation near the Ag-active surface. Nevertheless, SERR spectroscopy with variable excitation has proved to be a powerful tool in detecting the trace levels (down to 17 ppb vanadium and less than 10 ppb of nickel) of both VO(DPEP) and Ni(DPEP) in aqueous surfactant media.

Obtaining such information is of particular importance in the analysis of waters that have been in contact with high spills of crude oil with high metal content and related organic rich sediments. The authors have recently collected water samples from various natural aquatic sites near the petroleum industrial parks in Texas; while the SERR data remain to be acquired, these samples showed the presence of nickel and vanadium by ICP analyses but not IC. Since, as was shown in the present work, this partitioning is likely to be very low without the addition of a surfactant, the presence of these metals in the water phase at elevated levels (vanadium at 14−41 ppb and nickel at 42−86 ppb) is of interest. It is possible that dissolved humic and fulvic acids from soil and aquatic origins may be responsible for the enhanced solubilization of the nickel and vanadium complexes, similarly as reported by Chiou and colleagues (*46*, *47*) for the solubility enhancement of organic contaminants with a high K_{ow}.

The results presented here show an enhanced partitioning of nickel and vanadium porphyrins from the oil phase into the water phase when using surfactants. While the removal of only 0.01% of the metals during the short-term aqueous phase contact may not be significant for a remediation technique, it does point out that consideration should be given to this enhanced solubilization when using surfactant-enhanced remediation techniques at sites where a crude oil with a high trace metal content may be involved. Followup experiments with humic substances seem warranted.

Acknowledgments

We thank Mr. Alejandro Paquin of Petroleos de Venezuela and the Savannah Georgia CITGO refinery for providing the Boscan crude oil. This work was made possible by funding provided by the Teresa Heinz Environmental Scholars for Environmental Research (to J.R.S.), the Houston Area Molecular Biophysics Training Program (to R.C.), and the Robert A. Welch Foundation Grant E-1184 (to R.S.C).

Supporting Information Available

Additional text and two figures (9 pages). This material is available free of charge via the Internet at http://pubs.acs.org.

Literature Cited

(1) Al-Sulaimi, J.; Viswanathan, M. N.; Szekely, F. *Environ. Geol.* **1993**, *22*, 246.
(2) Baedecker, M. J.; Cozzarelli, I. M.; Eganhouse, R. P. *Appl. Geochem.* **1993**, *8*, 569.
(3) Speight, J. G. *The Chemistry and Technology of Petroleum*; Marcel Dekker: New York, 1991.
(4) Lysenko, S. V.; Norol'kov, N. S.; Karakhanov, E. A. *Pet. Chem., USSR* **1988**, *28*, 110.
(5) Abu-Elgheit, M. A.; El-Gayar, M. S.; Hegazi, A. H. Removal of Aromatics, Sulfur and Olefins. In *Gasoline and Diesel Symposia*, Ireland, FL, 1996; pp 632−636.
(6) Barakat, A. O.; Omar, M. F.; Scholz-Bottcher, B. M.; Rullkotter, J. Sulfur and Olefins. In *Gasoline and Diesel Symposia*, Ireland, FL, 1996; pp 637−641.
(7) Milgrom, R. *The Colors of Life. An Introduction to the Chemistry of Porphyrins and Related Compounds*; Oxford University Press: New York, 1997.
(8) Hodgson, G. W.; Baker, B. L.; Peake, E. In *Geochemistry of Porphyrins*; Nagy, B., Colombo, U., Eds.; Elsevier: Dordrecht, The Netherlands, 1967.
(9) Baker, E. W.; Palmer, S. E. In *The Porphyrins I*; Dolphin, D., Ed.; Academic Press: New York, 1978; pp 486−552.
(10) Treibs, A. *Angew. Chem.* **1936**, *49*, 682.
(11) Chicarelli, M. I.; Eckardt, C. B.; Owen, C. R.; Maxwell, J. R.; Eglinton, G.; Hutton, R. C.; Eaton, A. N. *Org. Geochem.* **1990**, *15*, 267.
(12) Dunning, H. N.; Moore, J. W.; Bieber, H.; Williams, R. B. *J. Chem. Eng. Data* **1960**, *5*, 546.
(13) Sugihara, J. M.; Bean, R. M. *J. Chem. Eng. Data* **1962**, *7*, 269.
(14) Viswanathan, M. N., Kuwait Institute for Scientific Research (KISR), personal communication, 1996.
(15) Lyman, W.; Reehl, W. F.; Rosenblatt, D. H. *Handbook of Chemical Property Estimation Methods, Environmental Behavior of Organic Compounds*; American Chemical Society: Washington, DC, 1990.
(16) Reinhard, M.; Drefahl, A. *Handbook for Estimating Physicochemical Properties of Organic Compounds*; John Wiley & Sons: New York, 1999.
(17) Rankin, J. G.; Czernuszewicz, R. S. *Org. Geochem.* **1993**, *20*, 521.
(18) Rankin, J. G.; Czernuszewicz, R. S.; Lash, T. D. *Org. Geochem.* **1995**, *23*, 419.
(19) Rankin, J. G.; Czernuszewicz, R. S.; Lash, T. D. *Inorg. Chem.* **1995**, *34*, 3025.
(20) Czernuszewicz, R. S.; Rankin, J. G.; Lash, T. D. *Inorg. Chem.* **1996**, *35*, 199.
(21) Rankin, J. G.; Cantú, R.; Czernuszewicz, R. S.; Lash, T. D. *Org. Geochem.* **1999**, *30*, 201.
(22) Fleischmann, M.; Hendra, P. J.; McQuillan, A. J. *J. Chem. Phys. Lett.* **1974**, *26*, 163.
(23) Woolley, P. S.; Brown, M. D.; Naylor, C. C.; Hester, R. E.; Keely, B. J. *Org. Geochem.* **1998**, *29*, 1063.
(24) Li, W.; Lash, T. D. *Tetrahedron Lett.* **1998**, *39*, 8571−8574.
(25) Lash, T. D.; Quizon-Colquitt, D. M.; Shiner, C. M.; Nguyen, T. H.; Hu, Z. *Energy Fuels* **1993**, *7*, 172.

(26) Quizon-Colquitt, D. M.; Lash, T. D. *J. Heterocycl. Chem*. **1993**, *30*, 477.
(27) Adler, A. D.; Longo, F. R.; Kampas, F.; Kim, J. *J. Inorg. Nucl. Chem*. **1970**, *32*, 2443.
(28) Smith, R. E. *Ion Chromatography Applications*; CRC Press: Boca Raton, FL, 1988.
(29) Takaya, M.; Sawatari, K. *Ind. Health* **1994**, *32*, 165.
(30) Stencel, J. R.; Jaffé, P. R. *First International Conference on Oil and Hydrocarbon Spills, Modelling, Analysis and Control*, Southampton, UK, 1998; pp 223−230.
(31) Schneider, S.; Halbig, P.; Grau, H.; Nickel, U. *Photochem. Photobiol.* **1994**, *60*, 605.
(32) Czernuszewicz, R. S. In *Methods in Molecular Biology*; Jones, C., Mulloy, B., Thomas, A. H., Eds.; Humana Press: Totowa, NJ, 1993; Vol. 17, pp 345−374.
(33) Gouterman, M. In *The Porphyrins I*; Dolphin, D., Ed.; Academic Press: New York, 1978; pp 1−165.
(34) Medforth, C. J.; Senge, M. O.; Smith, K. M.; Sparks, L. D.; Shelnutt, J. A. *J. Am. Chem. Soc.* **1992**, *114*, 9859.
(35) Prendergast, K.; Spiro, T. *J. Am. Chem. Soc.* **1992**, *114*, 3793.
(36) Guha, S.; Jaffé, P. *Environ. Sci. Technol.* **1996**, *30*, 605.
(37) Guha, S.; Jaffé, P. R. *Environ. Sci. Technol.* **1998**, 32, 930.
(38) Su, Y. O.; Czernuszewicz, R. S.; Miller, L. A.; Spiro, T. G. *J. Am. Chem. Soc.* **1988**, *110*, 4150.
(39) Van Berkel, G. J.; Quirke, J. M. E.; Filby, R. H. *Org. Geochem*. **1989**, *14*, 129.
(40) Vickova, B.; Matejka, P.; Simonova J.; Cermakova, K.; Pancoska, P.; Baumruk, V. *J. Phys. Chem*. **1993**, *97*, 9719.
(41) Woolley, P. S.; Keely, B. J.; Hester, R. E. *J. Chem. Soc., Perkin Trans.* **1997**, *2*, 1731.
(42) Pettersen, R. C. *Acta Crystallogr. Sec. B.* **1969**, *25*, 2527.
(43) Pettersen, R. C. *J. Am. Chem. Soc.* **1971**, *93*, 5629.
(44) Scheidt, W. R. In *The Porphyrins III*; Dolphin, D., Ed.; Academic Press: New York, 1978; pp 463−511.
(45) Yan, Q. Ph.D. Dissertation, University of Houston, 1995.
(46) Chiou, C. T.; Malcom, R. L.; Brinton, T. I.; Kile, D. E. *Environ. Sci. Technol.* **1986**, *20*, 502.
(47) Chiou, C. T.; Kile, D. E.; Brinton, T. I.; Malcom, R. L. Leenher, J. A. *Environ. Sci. Technol.* **1987**, *21*, 1231.
(48) Li, X.-Y.; Czernuszewicz, R. S.; Kincaid, J. R.; Stein, P.; Spiro, T. G. *J. Phys. Chem*. **1990**, *94*, 47.
(49) Li, X.-Y.; Czernuszewicz, R. S.; Kincaid, J. R.; Su, Y. O.; Spiro, T. G. *J. Phys. Chem*. **1990**, *94*, 31.

Received for review February 23, 1999. Revised manuscript received October 1, 1999. Accepted October 5, 1999.

ES990213S